Experimental ionization-rate coefficients for hydrogenlike, heliumlike, and lithiumlike ions

P. Greve, M. Kato, H.-J. Kunze, and R. S. Hornady*
Institut für Experimentalphysik V, Ruhr-Universität, 4630 Bochum, West Germany
(Received 9 December 1980)

Electron-impact ionization-rate coefficients are obtained for lithiumlike, heliumlike, and hydrogenlike ions by the plasma spectroscopy method. The plasma is produced in a 140-kJ large-bore theta pinch, and electron density and temperature are determined by 90° Thomson scattering. The basic requirements of the evaluation technique employed are briefly discussed and the results are compared with other measurements and theoretical calculations.

I. INTRODUCTION

Recent advances in the production and studies of high-temperature plasmas in controlled nuclear fusion research point out the continuing need for rate coefficients for ionization of highly charged ions; they are needed not only for diagnostic purposes but also for modeling the impurity transport, for calculation of radiation losses, and for determining various plasma properties.

Two methods have been successful for multiple charged ions: the crossed-beams method and the plasma spectroscopy method.

The first one yields the cross sections over a wide range of electron energies, is capable, in principle, of good accuracy, and allows detailed comparisons with theoretical calculations. Due to the lack of suitable ion beams, experimental observations have been limited so far to ions of charge state less than five.[1,2] The plasma spectroscopy method[3] yields effective rate coefficients, i.e., the quantities usually needed in the applications, and is not limited to lower charge states.[4] In this paper, rate coefficients for hydrogenlike, heliumlike, and lithiumlike ions obtained by this method are reported. They are compared with other available theoretical and measured values.

II. THE PLASMA SPECTROSCOPY METHOD

The method has been described previously,[7] and Refs. 4 to 13 cover all measurements of ionization rates reported so far. Therefore, we shall not describe the technique in detail, but summarize briefly some essential assumptions and basic requirements for the evaluation of the rate coefficients from the observations as well as point out limitations to this method imposed by experimental conditions which could lead to systematic errors.

In this experiment, as well as in most of the others, the elements of interest are added in small amounts to the initial filling gas, usually hydrogen, of a theta pinch. As the gas is ionized, compressed, and heated very rapidly to high temperatures, the impurity atoms go through the ionization stages successively, their time histories being governed by the ionization rates as long as recombination can be neglected. In this way, experimentally obtained time histories allow the derivation of the ionization rates if plasma density and temperature as well as the time evolution of the plasma volume in the direction of observation are known.

The quantities actually observed are the intensities of lines as function of time emitted by the ions, although no absolute values are required. The choice of suitable transitions facilitates the analysis. Lines whose upper levels are populated by a dipole transition from the ground state have the advantage that the temperature dependence of the excitation rate coefficient is fairly well known,

$$X \sim \frac{1}{\sqrt{kT_e}} \exp\left(-\frac{\Delta E}{kT_e}\right), \tag{1}$$

where ΔE is the excitation energy. (The weak dependence of the effective Gaunt factor on the temperature is neglected.) The intensity P of such a line is then given by

$$P = \int \epsilon \, ds = \frac{h\nu}{4\pi} A \int N_j(u) \, ds \,, \tag{2}$$

or, for a homogeneous plasma of length L along the line of sight s, by

$$P = \text{const} \times N_j(g) N_e \frac{L}{\sqrt{kT_e}} \exp\left(-\frac{\Delta E}{kT_e}\right). \tag{3}$$

ϵ is the emission coefficient, A is the transition probability, $h\nu$ is the photon energy, $N_j(u)$ and $N_j(g)$ are the population densities of upper level (u) and ground state (g), N_e is the electron density, and T_e is the electron temperature.

The time history is characterized by the logarithmic derivative

$$\frac{1}{P}\frac{dP}{dt}=\frac{1}{N_j(g)}\frac{dN_j(g)}{dt}+\frac{1}{N_e}\frac{dN_e}{dt}$$

$$+\left(\frac{\Delta E}{kT_e}-\frac{1}{2}\right)\frac{1}{kT_e}\frac{d(kT_e)}{dt}+\frac{1}{L}\frac{dL}{dt}. \qquad (4)$$

At low electron densities, the upper levels of the ion (j) are populated according to the coronal model and practically all ions are in the ground state; we may approximate $N_j(g)\simeq N_j$, where N_j now is the total density of this ionization stage.

These densities are governed by rate equations [Eqs. (3) of Ref. 3], and in the limit of negligible recombination Eq. (4) becomes

$$\frac{1}{P}\frac{dP}{dt}=\frac{N_{j-1}}{N_j}N_eI_{j-1}-N_eI_j+\frac{2}{N_e}\frac{dN_e}{dt}$$

$$+\left(\frac{\Delta E}{kT_e}-\frac{1}{2}\right)\frac{1}{kT_e}\frac{d(kT_e)}{dt}+\frac{1}{L}\frac{dL}{dt}, \qquad (5)$$

where I_j is the rate coefficient for ionization.

It is obvious that density variations affect the time histories most strongly, whereas temperature changes have little influence if a transition is selected having an excitation energy which is about one-half the electron temperature. The late-time decay of a line ($N_{j-1}\ll N_j$) is essentially determined by N_eI_j only and could thus yield I_j directly. Care must be exercised, however, since ions in the low density, cooler plasma outside the core may be responsible for long lasting tails (especially when observing end-on in a theta pinch) and thus lead to systematic errors. It is necessary, therefore, to use the complete time history of an ionization stage for the derivation of the desired rate coefficient. This is done by solving the coupled rate equations for the various ion densities, using measured electron density and temperature, and varying the assumed rate coefficients until computed and observed time histories match. Since spectroscopic observations integrate along the line of sight, the length of the observed plasma and its homogeneity must be known. Thomson scattering is usually done only along a diameter in the midplane of the theta-pinch coil yielding this information there, but corresponding measurements along the axis are omitted because they are either too cumbersome or not possible for experimental reasons. In many cases, it may be sufficient to measure the length L of the plasma column, by observing the continuum radiation or suitable lines through holes in the pinch coil, and then to correct for changes in L. This has to be done also for side-on observations as well since the varying magnetic field results in non-negligible variations of the plasma diameter even in the quiescent phase of the discharge.

The operation of the discharge without reversed-bias field is not recommended as detailed light scattering measurements along the axis and even outside the coil reveal that density pulses traveling along the field lines may occur resulting in strong axial inhomogeneities.[14] To reduce these problems, a small magnetic field opposite to the direction of the main field usually is applied to the preheated plasma. During the implosion, field lines connect forming a hot annulus, which is compressed radially and axially; most observations indicated that the length of this annulus remains fairly constant for sufficiently long times. At low plasma densities such a trapped magnetic field could influence, on the other hand, the distribution of the ionization stages within the plasma if the ion Larmor radius becomes small, because the ionization will then be more rapid in the high-density annulus than in the plasma region having the trapped magnetic field. However, at the densities of our pinch discharge, the impurity ions diffuse rapidly through collisions with the protons rather than gyrating around the trapped magnetic field lines.

For several reasons it is advisable, therefore, to perform observations of the time histories end-on as well as side-on; if they yield identical results several sources of systematic errors are excluded. In all other cases, the optical depth τ of the lines observed must be checked if they terminate at lower levels which are populated strongly. The optical depth is given by[15]

$$\tau=3.0\times10^{-9}\left(\frac{AE_H}{kT_j}\right)^{1/2}fN_j(l)\lambda L, \qquad (6)$$

where f is the absorption oscillator strength, $N_j(l)$ is the population density of the lower level (l), A is the atomic weight, E_H is the ionization energy of hydrogen, λ is the wavelength in cm, and kT_j is the kinetic temperature of the ion. kT_j can be estimated from the width of Doppler broadened lines in the visible spectral region. If this is not possible, one preferably checks the optical depth experimentally by observing the time histories and the absolute intensities of the lines for various impurity concentrations. The $2s$-$2p$ resonance transitions of the lithiumlike ionization stage should be the ones with the largest τ, and if their time histories are not influenced by optical depth effects (checked easily by comparison with the $3s$-$3p$ transitions of the same ionization stage), the optical depth will also be small enough for most other transitions.

The quantities obtained are rate coefficients, i.e., the cross section times the electron velocity averaged over the velocity distribution function. In most cases, this distribution function is Maxwellian, deviations being observed only at early

times of a discharge[16] or during strong ionization of the fill gas.[17] The measured coefficients actually represent effective rate coefficients which include ionization from excited states as well as from inner shells; however, under suitable conditions these contributions are negligible.

Finally, the initial distribution of the ionization stages after formation of the hot plasma should be commented on. The computer modeling of the ions assumes a homogeneous transient plasma, which is in contrast to the early very dynamic phase of the theta-pinch discharge; this is characterized by large density and temperature inhomogeneities over the cross section of the plasma. The experimental determination of the initial ion distribution thus poses a formidable task. In practice, however, this is not necessary. The initial distribution is simulated by "fictitious ionization-rate coefficients" which are chosen to match computed and observed time histories of the first ionization stages; they have no physical meaning but simply model the initial situation. The following ionization stages in the quiescent phase of the discharge are then described by their actual rate coefficients.

III. EXPERIMENTAL SETUP

The plasma was generated in a theta pinch, which has been constructed specifically for spectroscopic measurements. A 60 cm-long coil with an inner diameter of 21 cm is fed via a vertical collector plate from three capacitor banks standing on a scaffold. In this way measurements from all sides were possible. A schematic of the overall arrangement is shown in Fig. 1.

A discharge cycle is initiated by an HF discharge which produces the first electrons and thus assures reproducibility. Bias, preheater, and main bank are discharged in sequence. Two conditions were investigated, the discharge-circuit parameters being shown in Table I. The main discharge is crowbarred at the time of maximum current; in this way, the lifetime of the hot plasma is prolonged. End-on framing pictures, as well as side-on streak pictures, show that the hot annulus exists for about 10 μs, after which it decays by a rotational instability.

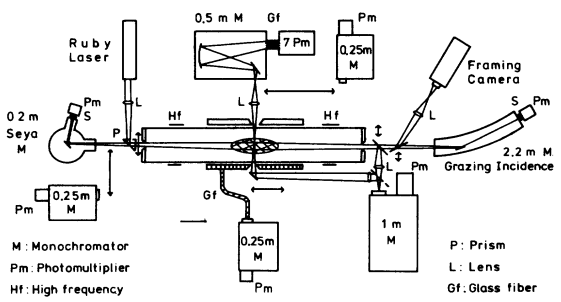

FIG. 1. Schematic overview of the experimental setup.

TABLE I. Discharge circuit parameters.

Condition			I	II
Filling pressure H_2 (mTorr)			20	12
Biasbank	charging voltage	(kV)	8	4
	stored energy	(kJ)	4	1
	quarter period	(μs)	42	42
Preheater	charging voltage	(kV)	46	46
	stored energy	(kJ)	2	2
	quarter period	(μs)	1.5	1.5
Mainbank	charging voltage	(kV)	35	35
	stored energy	(kJ)	55	110
	quarter period	(μs)	4.5	5.7

The length of the plasma column is determined from the continuum radiation in the visible spectral region which is observed through small holes of 1-mm diameter along the axis of the discharge coil. Each discharge is monitored in two ways: the continuum intensity at 5226 Å is observed side-on, and the dI/dt of the discharge current is recorded by an eight-meter-long Rogowski coil placed around one of the collector plates.

For Thomson scattering, the 200-MW beam from a ruby laser is focused parallel to the axis of the discharge tube in the midplane of the coil. The focus of 4-mm diameter can be scanned radially. The scattered light is observed at 90° and analyzed using a 0.5-m monochromator equipped with a seven-channel glass fiber photomultiplier system. Two vacuum-uv monochromators are used for end-on observations of the line radiation and several monochromators for the visible spectral region for side-on as well as end-on measurements.

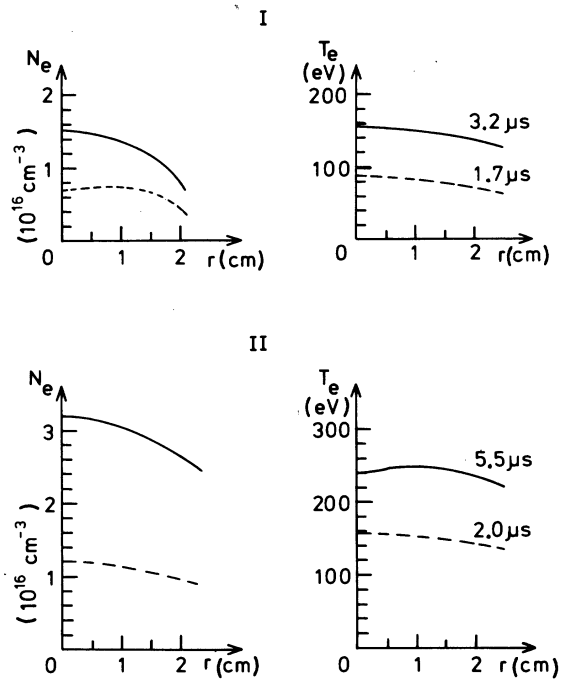

FIG. 2. Radial electron density and temperature distribution at two times for conditions I and II.

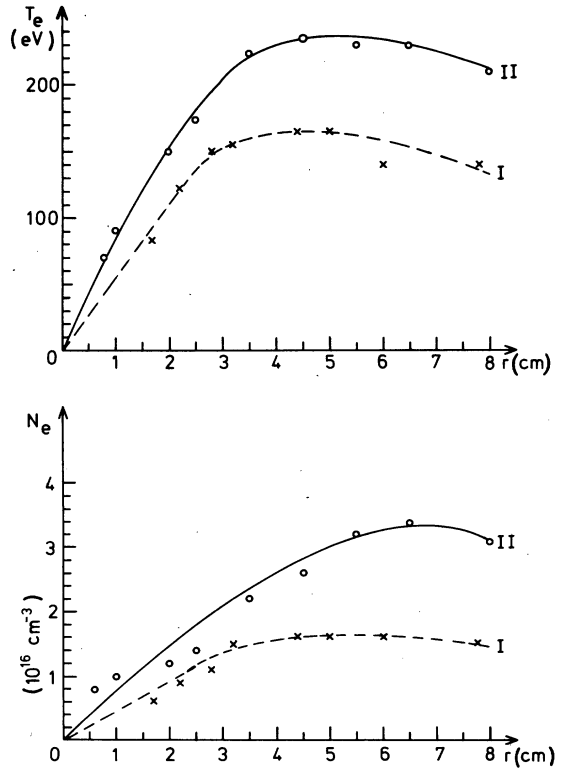

FIG. 3. Average electron density and temperature as function of time for conditions I and II.

TABLE II. Observed spectral lines.

Ion	Transition	Wavelength (Å)	s: side-on e: end-on
B II	$1s^2 2s^2\,{}^1S$-$2s2p\,{}^1P^o$	1362.5	e
	$2s^2\,{}^1S$-$2s3p\,{}^1P^o$	693.95	e
	$2s2p\,{}^1P^o$-$2p^2\,{}^1D$	3451.3	e,s
III	$1s^2 2s\,{}^2S$-$2p\,{}^2P^o$	2065.8	e,s
		2076.2	
	$2s\,{}^2S$-$3p\,{}^2P^o$	518.2	e
	$4f\,{}^2F^o$-$5g\,{}^2G$	4497.6	s
IV	$1s^2\,{}^1S$-$1s2p\,{}^1P^o$	60.3	e
	$1s2s\ S$-$1s2p\,{}^3P^o$	2826.7	e,s
		2822.6	
V	$1s\,{}^2S$-$2p\,{}^2P^o$	48.6	e
	$1s\,{}^2S$-$3p\,{}^2P^o$	41.0	e
	$2p\,{}^2P^o$-$3d\,{}^2D$	262.4	e
C III	$1s^2 2s^2\,{}^1S$-$2s2p\,{}^1P^o$	977.03	e
	$2s2p\,{}^1P^o$-$2p^2\,{}^1D$	2296.9	e,s
	$2s2p\,{}^3P^o$-$2p^2\,{}^3P$	1175.7	e
IV	$1s^2 2s\,{}^2S$-$2p\,{}^2P^o$	1548.2	e
		1550.8	
	$2s\,{}^2S$-$3p\,{}^2P^o$	312.4	e
	$3s\,{}^2S$-$3p\,{}^2P^o$	5801.3	s
		5812.0	
V	$1s^2\,{}^1S$-$1s2p\,{}^1P^o$	40.3	e
	$1s2p\,{}^1P^o$-$1s3d\,{}^1D$	267.3	e
	$1s2s\,{}^3S$-$1s2p\,{}^3P^o$	2270.9	e,s
		2277.9	
VI	$1s\,{}^2S$-$2p\,{}^2P^o$	33.7	e
	$1s\,{}^2S$-$3p\,{}^2P^o$	28.5	e
	$2p\,{}^2P^o$-$3d\,{}^2D$	182.2	e
N IV	$1s^2 2s^2\,{}^1S$-$2s2p\,{}^1P^o$	765.1	e
	$2s^2\,{}^1S$-$2s3p\,{}^1P^o$	247.2	e
	$2s3s\,{}^3S$-$2s3p\,{}^3P^o$	3478.7	s
		3484.9	
V	$1s^2 2s\,{}^2S$-$2p\,{}^2P^o$	1238.8	e
		1242.8	
	$2s\,{}^2S$-$3p\,{}^2P^o$	209.3	e
	$3s\,{}^2S$-$3p\,{}^2P^o$	4603.8	s
		4620.0	
VI	$1s^2\,{}^1S$-$1s2p\,{}^1P^o$	28.8	e
	$1s2s\,{}^3S$-$1s2p\,{}^3P^o$	1896.8	e
		1907.7	
O V	$1s^2 2s^2\,{}^1S$-$2s2p\,{}^1P^o$	629.7	e
	$2s^2\,{}^1S$-$2s3p\,{}^1P^o$	172.2	e
	$2s3s\,{}^1S$-$2s3p\,{}^1P^o$	5114.2	s
VI	$1s^2 2s\,{}^2S$-$2p\,{}^2P^o$	1031.9	e
		1037.6	
	$2p\,{}^2P^o$-$3d\,{}^2D$	173.0	e
	$3s\,{}^2S$-$3p\,{}^2P^o$	3811.3	s
		3834.2	
VII	$1s2p\,{}^1P^o$-$1s3d\,{}^1D$	135.8	e
F V	$1s^2 2s^2 2p\,{}^2P^o$-$2s2p^2\,{}^2D$	654.0	e
		657.3	

TABLE II. (*Continued*)

Ion	Transition	Wavelength	*s*: side-on *e*: end-on
VI	$1s^2 2s^2\,{}^1S$-$2s2p\,{}^1P^o$	535.2	*e*
	$2s2p\,{}^1P^o$-$2p^2\,{}^1D$	1139.5	*e*
VII	$1s^2 2s\,{}^2S$-$2p\,{}^2P^o$	883.1	*e*
		890.8	
	$3s\,{}^2S$-$3p\,{}^2P^o$	3246.6	*s*
		3276.6	
Ne VI	$1s^2 2s^2 2p\,{}^2P^o$-$2s2p^2\,{}^2S$	433.2	*e*
		453.7	
VII	$1s^2 2s^2\,{}^1S$-$2s2p\,{}^1P^o$	465.2	*e*
	$2s^2\,{}^1S$-$2s3p\,{}^1P^o$	97.5	*e*
VIII	$1s^2 2s\,{}^2S$-$2p\,{}^2P^o$	770.4	*e*
		780.3	
	$2s\,{}^2S$-$3p\,{}^2P^o$	88.1	*e*
	$3s\,{}^2S$-$3p\,{}^2P^o$	2860.1	*s*

IV. RESULTS AND DISCUSSION

A. Experimental conditions

The pinch discharge was operated at two different conditions: 20-mTorr filling pressure and 55-kJ main-bank energy, and 12-mTorr filling pressure and 110-kJ main-bank energy (see Table I). For condition I only one-half of the units of the main bank was connected to the collector plates, the reverse bias field being about $0.08T$. Both conditions yielded stable plasmas. The impurities were added as gas admixtures of about 1% partial pressure to the initial hydrogen filling.

Figure 2 shows radial electron density and temperature distributions at two different times for both conditions as obtained from Thomson scattering. For the solution of the coupled rate equations, values averaged over the column cross section are used, and their time dependence is shown in Fig. 3. The radial homogeneity was good in both cases after 2 μs. The continuum radiation observed side-on revealed that the length of the plasma column remained constant to within 15% from 2 μs to over 10 μs.

For both conditions spectral lines from various ionization stages of the elements boron, carbon, nitrogen, oxygen, fluorine, and neon were observed; the transitions are listed in Table II. The last column indicates whether the observations were made end-on (*e*) or side-on (*s*). For most ions, comparison of end-on and side-on observations was possible, thus verifying that the time histories of lines from the same ionization stage are identical to within 10%. In this way, the long lasting tail observed in the spectral emission of some early ionization stages due to end losses or colder plasma regions outside the hot core could be identified and thus neglected.

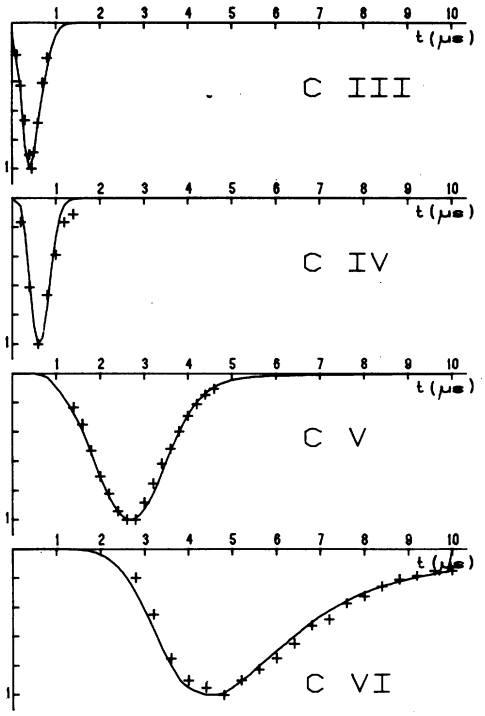

FIG. 4. Computed time histories of carbon ions (full lines) matched to observed ones (crosses) for condition II.

Figure 4 shows one example of computed time histories matched to observed ones (crosses) for the case of carbon ions in the plasma produced under condition II. The intensities are normalized to their peak values before comparison is made.

TABLE III. Collisional ionization-rate coefficients for hydrogenlike ions in units of 10^{-11} cm^3 s^{-1}.

Ion	kT_e (eV)	kT_e/E_i[a]	N_e (10^{16} cm^{-3})	ECIP	GS	Lotz	Y	Expt
B V	230	0.68	2.6	5.6	5.8	6.0	5.3	5.3
C VI	230	0.47	3.2	1.5	1.6	1.6	1.4	1.5

[a] E_i is the ground-state ionization potential.

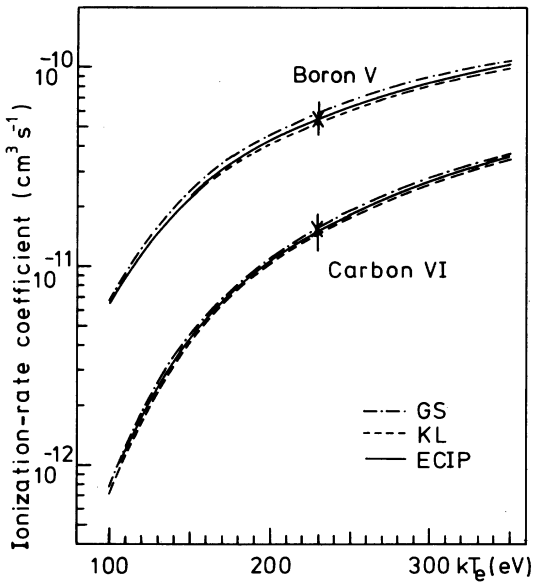

FIG. 5. Ionization-rate coefficients for B V and C VI as a function of temperature. Crosses are present data; solid curve, ECIP from Ref. 19; dot-dashed curve, from Ref. 20; dashed curve (KL), calculated according to the semiempirical formula of Ref. 7, which approximates the values of Lotz (Ref. 18) to better than 15%.

The early ionization stages are matched by "fictitious coefficients" as discussed in Sec. II, and only the rate coefficients for C V and C IV are given as results because these ions occur during the quiescent phase of the discharge. The accuracy of the best fit was checked by varying the rate coefficients used. In all cases, a variation of 20% resulted in distinguishable differences between experimental and computed time histories. Taking into account the uncertainty of the density measurement, the error of the rate coefficients determined is estimated to about 25%. Fifteen rate coefficients were thus deduced, and the results will be discussed in the following subsections.

B. Hydrogenic ions

Two ions of the hydrogen isoelectronic sequence were observable for sufficiently long times given the higher density and higher temperature of condition II. Table III gives the experimental results. They are compared with semiempirical values predicted by Lotz,[18] with values obtained according to the semiclassical calculation (ECIP) introduced by Burgess,[19] and with theoretical calculations of Golden and Sampson[20] using the Born exchange approximation (GS) and of Younger[21] using a distorted-wave approximation (Y). The agreement between experiment and predicted theoretical values is excellent; the deviations do not exceed 10%. Figure 5 shows the temperature dependence of the rates and the experimental values.

C. Heliumlike ions

Ions of the helium-isoelectronic sequence are characterized by a high-lying metastable level resulting in a sufficiently strong population of the $n = 2$ triplet levels for additional ionization from these levels to become important in laboratory plasmas. If the notation of Refs. 6 and 10 is used, the effective ionization coefficient for a heliumlike ion may be written

$$I_{\mathrm{eff}} = (I_1 + \alpha X_{31}), \tag{7}$$

where I_1 describes the ionization from the ground state, X_{31} is the excitation rate coefficient to the $n = 2$ triplet states from the ground state, and α is the branching ratio for ionization from these levels. This ratio is temperature as well as density dependent, and measurements of the effective ionization rate, especially at very different plasma densities, would thus yield useful information on α. In practice, however, this is not achievable with the one pinch device, although some range of α may be covered by simply investigating different ions, as will be seen below.

Table IV gives results for B IV, C V, and N VI

TABLE IV. Collisional rate coefficients for heliumlike ions in units of 10^{-10} $cm^3 s^{-1}$.

Ion	kT_e (eV)	kT_e/E_i	N_e (10^{16} cm^3)	α	$[\alpha X_{31}]_1$	$[\alpha X_{31}]_2$	Ionization-rate coefficients ECIP	GS	Lotz	Y	I^{cr}_{expt}	$I_{eff\,1}$	$I_{eff\,2}$	$I_{eff\,expt}$
B IV	140	0.54	1.3	0.68	0.77	0.38	1.17	1.00	1.18	0.98	0.93	1.75	1.36	1.64
B IV	175	0.67	1.4	0.71	0.99	0.46	1.82	1.55	1.80	1.53	1.47	2.52	1.99	2.02
C V	160	0.41	1.6	0.53	0.25	0.21	0.32	0.28	0.32	0.26	0.24	0.51	0.47	0.44
C V	210	0.54	2.2	0.60	0.38	0.30	0.63	0.54	0.62	0.53	0.50	0.91	0.80	0.75
N VI	235	0.43	2.6	0.31	0.10	0.07	0.21	0.19	0.21	0.18	0.23	0.28	0.25	0.24
C V[a]	240	0.61	0.65	0.48	0.35	0.25	0.83	0.71	0.82	0.69	0.68	1.04	0.94	0.90

[a] From Ref. 6.

obtained under the two plasma conditions. The last column $I_{\text{eff expt}}$ shows the effective ionization-rate coefficients measured. For comparison, again four theoretical or semiempirical values for the ionization from the ground state are listed. These agree with each other to within 15%. The column Y contains the values from Ref. 22, where other theoretical calculations also are discussed.

The branching ratio α is calculated according to Refs. 10 and 23 and varies from 0.3 for NVI to 0.7 for BIV. In the two cases of BIV the radiative depopulation of the triplet levels is 2% or less of the collisional depopulation and thus negligible,

$$\alpha = \frac{I_3 N_e}{A_{13} + (I_3 + X_{3\geqslant})N_e} \simeq \frac{1}{1 + X_{3\geqslant}/I_3}, \tag{8}$$

α thus being determined solely by the assumed ratio of collisional transfer rate coefficient $X_{3\geqslant}$ from the $n=2$ triplet levels to singlet levels of $n=3$ and higher and the $n=2$ triplet level ionization coefficient I_3. For the case of NIV, radiative and collisional rates are of equal magnitude. The absolute contribution αX_{31} to the ionization is estimated in two ways. In column $[\alpha X_{31}]_1$ the rate coefficient X_{31} was taken to be $X_{21}/1.8$, where X_{21} is the total excitation coefficient to the $n=2$ singlet levels calculated in the effective Gaunt-factor approximation. This was found to be consistent with experimental observations.[6,23,24] The total effective rate coefficients obtained using the ground-state ionization value of Younger[22] (column Y) are shown in column I_{eff1}. If we compare these with the experimental values of the last column, we find the experimental results to be ~85% of the theoretical estimates. This agreement is satisfactory, but as Table IV shows, the contribution $[\alpha X_{31}]_1$ to the total ionization varies from 35% to nearly 50%, and I_{eff} is thus strongly influenced by X_{31}. For this reason, $[\alpha X_{31}]_2$ was estimated also using recent calculations of van Wyngaarden *et al.*[25] who obtained excitation rates using close-coupling calculations. Their values do not include cascading contributions which can be substantial for the population of the $n=2$ triplet levels. Following the discussion of Ref. 26, we add 30% cascading contributions, although this could be still an underestimate.[23] The effective rate coefficients thus obtained are listed in column I_{eff2}. The mean deviation between theoretical and experimental values now is negligibly small, thus the agreement is very satisfactory. However, the analysis reveals the uncertainty in the derivation of the ground-state ionization coefficients. Independent measurements of α and X_{31} are desirable as well as measurements at very low densities, where αX_{31} becomes negligible. If the first estimate of $[\alpha X_{31}]_1$ would be exactly correct, the deduced ground-state ionization coefficients are 75% of the theoretical values (Y or GS) on the average. These results are consistent with earlier measurements using the same technique.[6,10] Column $I^{\text{cr}}_{\text{expt}}$ shows, for comparison, rate coefficients derived from cross sections obtained using the crossed-beams technique by Crandall *et al.*[1]

D. Lithiumlike ions

Ions of the lithium isoelectronic sequence have been studied most extensively so far. Table V shows our present experimental results (accuracy ±25%), theoretical values as well as the rate coefficients from the crossed-beams technique $I^{\text{cr}}_{\text{eff}}$ (see Refs. 1, 26, 27, 28). The theoretical rates are ground-state ionization rates and do not include contributions due to excitation-autoionization as well as ionization from excited levels. For our plasma conditions, ionization from the $2p$ levels will contribute and increase the effective ionization rates above the pure ground-state rates.[7] Since the population of the $2p$ levels can be calculated rather accurately[23] (it varies between 25% and 46% of the total population for the different ions and different plasma conditions), this relative increase is derived using the analytic ionization formula of Ref. 7. If we introduce $N(2p)/N(2s)=\beta$, the effective rate [Eq. (6) of Ref. 7] may be written as

TABLE V. Collisional ionization-rate coefficients for lithiumlike ions in units of 10^{-10} cm^3 s^{-1}.

Ion	kT_e (eV)	kT_e/E_i	N_e (10^{16} cm^3)	ECIP	GS	Lotz	Y	$I^{\text{cr}}_{\text{expt}}$	$I_{\text{eff expt}}$	$I_{\text{1 eff}}/I_1$	$I_{\text{1 expt}}$	$I_{\text{1 expt}}$/GS
N V	110	1.12	0.8	3.98	5.76	7.77	6.21	6.65	4.40	1.12	3.93	0.68
N V	120	1.23	1.1	4.39	6.23	8.50	6.77	7.27	4.00	1.13	3.54	0.57
O VI	135	0.98	1.2	2.01	3.10	3.96	3.30	3.77	2.24	1.09	2.06	0.66
O VI	160	1.16	1.3	2.47	3.69	4.80	3.92	4.57	2.70	1.09	2.48	0.67
F VII	160	0.86	1.5	1.09	1.78	2.20	1.83		1.43	1.06	1.35	0.76
F VII	180	0.97	1.5	1.29	2.05	2.56	2.12		1.43	1.06	1.35	0.66
Ne VIII	160	0.67	1.8	0.49	0.86	1.10	0.86		0.51	1.05	0.49	0.57
Ne VIII	220	0.92	2.2	0.82	1.34	1.62	1.37		0.76	1.05	0.72	0.54

$$\frac{I_{\mathrm{eff}}}{I_1} = \frac{1}{1+\beta}\left(1+\beta\,\frac{I(2p)}{I_1}\right), \tag{9}$$

where $I(2p)$ is the ionization-rate coefficient from the $2p$ levels. Thus, the proper correction factor is used to derive the ground-state rate coefficient $I_{1\,\mathrm{expt}}$ from $I_{\mathrm{eff\,expt}}$. Contributions from higher excited levels are neglected, which seems justified according to the analysis of Ref. 13 for our ions and values of kT_e/E_i.

The self-consistency of the results between the various ions in the temperature range $0.67 \leq kT/E_i < 1.23$ is very good. This is evident if we calculate the average ratio of the experimental values and those of Golden and Sampson (GS), for example. We obtain

$$\langle I_{1\,\mathrm{expt}}/I_{\mathrm{GS}}\rangle = 0.64 \pm 0.03\,;$$

the rms deviation is less than 5%. The average agreement again is best with the ECIP results:

$$\langle I_{1\,\mathrm{expt}}/I_{\mathrm{ECIP}}\rangle = 1.00 \pm 0.05\,.$$

This confirms previous conclusions (see Refs. 2 and 10).

The above discrepancy between theory (GS) and experiment could be reduced by decreasing the ionization from the $2p$ levels relative to that from the ground state in the analysis [see Eq. (9)]. For the low-Z ions a reduction by a factor of about 5 would be required; for Ne VIII, however, even a negligible ionization from the $2p$ levels would not be sufficient. Such a reduction of the ratio $I(2p)/I(2s)$ is not consistent with theoretical calculations (see e.g., Ref. 20).

Figures 6(a) and 6(b), finally, illustrate the results; they show theoretical rate coefficients as well as all experimental values obtained by the same technique. The present results are consistent with other values[7] obtained in a somewhat smaller device. However, they do not agree with those of Refs. 12 and 13 measured by the same technique, although the value of Ne VIII of Ref. 11 again is in agreement, revealing some inconsistency along the isoelectronic sequence of the results obtained in the pinch discharge of Refs. 11 and 12. In contrast to these deviating pinch measurements, the time histories of spectral lines were observed side-on as well as end-on in the present experiments; it was possible thus to select extremely suitable plasma conditions where both time histories indeed were identical. This eliminated possible systematic errors caused, for example, by particle influx from outside the hot plasma or by plasma dynamics. The success of fitting computed time histories with the observations is illustrated in Fig. 4. Most puzzling is the disagreement with the results obtained by the crossed-beams technique, and it remains to be resolved why agreement is obtained for C IV and not for the other members of the sequence.

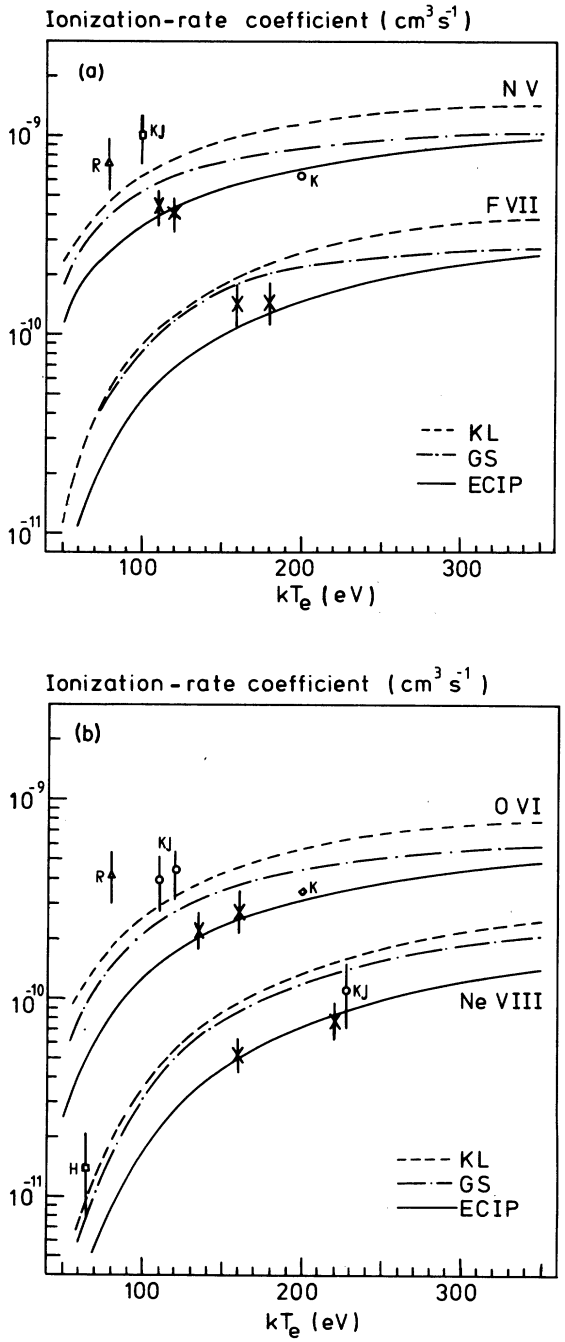

FIG. 6. Ionization-rate coefficients as function of temperature (a) for N V and F VII, (b) for O VI and Ne VIII. Crosses are present data, K from Ref. 7, KJ from Refs. 11 and 12, R from Ref. 13; solid curve, ECIP from Ref. 19; dot-dashed curve, from Ref. 20; dashed curve, from Ref. 7.

The neglect of impurity particles arriving from

cooler parts during the time of measurement is also supported by theoretical estimates which indicate, that for the most unfavorable conditions the time constant for particle influx is at least two orders of magnitude larger than the ionization times measured.

Hydrogenlike boron and lithiumlike neon have comparable ionization times and were measured under identical conditions in the same pinch discharge. Most conceivable systematic errors should have influenced, therefore, both rate coefficients in the same direction unless a physical process yet unknown is involved, which is operative only on ions with more than two electrons. Charge exchange with neutral hydrogen as cause of this discrepancy should be excluded for the same reasons, although the neutral hydrogen density in the hot plasma is not known.

V. CONCLUSIONS

Ionization-rate coefficients were measured for several ions with one, two, and three electrons. The results are in good agreement with theoretical calculations for hydrogenlike ions and heliumlike ions although in the latter case some ambiguity remains due to the step-wise ionization through the metastable triplet levels. For lithiumlike ions, however, the rate coefficients are 64% of theoretical calculations only. This discrepancy is manifested with great consistency along the isoelectronic sequence from NV to NeVIII; possible systematic errors are discussed and can be excluded.

ACKNOWLEDGMENTS

The authors wish to thank M. Blaha, H. R. Griem, and S. M. Younger for valuable discussions, G. Skopp and several members of the Institute for Plasmaphysics of the KFA Jülich for engineering assistance with the construction of the theta pinch, and N. Gramoschke and J. Semerad for their technical assistance in maintaining the experiment. This work was supported by the Deutsche Forschungsgemeinschaft. One of us (H.J.K.) was supported partly by the U. S. Department of Energy. Most of the capacitors were kindly provided by the KFA Jülich.

---

*Present address: Lawrence Livermore National Laboratory, Livermore, California 94550.

[1]D. H. Crandall, R. H. Phaneuf, and D. C. Gregory, Oak Ridge National Laboratory Report No. ORNL/TM-7020, (unpublished).
[2]A. Burgess, H. P. Summers, D. M. Cochrane, and R. W. P. McWhirter, Mon. Not. R. Astron. Soc. 179, 275 (1977).
[3]H.-J. Kunze, Space Sci. Rev. 13, 565 (1972).
[4]C. Breton, C. de Michelis, M. Finkenthal, and M. Mattioli, Phys. Rev. Lett. 41, 110 (1978).
[5]E. Hinnov, J. Opt. Soc. Am. 56, 1179 (1966); 57, 1392 (1968).
[6]H.-J. Kunze, A. H. Gabriel, and H. R. Griem, Phys. Rev. 165, 267 (1968).
[7]H.-J. Kunze, Phys. Rev. A 3, 937 (1971).
[8]R. U. Datla, H.-J. Kunze, and D. Petrini, Phys. Rev. A 6, 38 (1972).
[9]R. U. Datla, M. Blaha, and H.-J. Kunze, Phys. Rev. A 12, 1076 (1975).
[10]R. U. Datla, L. J. Nugent, and Hans R. Griem, Phys. Rev. A 14, 979 (1976).
[11]L. A. Jones, E. Källne, and D. B. Thomson, J. Phys. B 10, 187 (1977).
[12]E. Källne and L. A. Jones, J. Phys. B 10, 3637 (1977).
[13]W. L. Rowan and J. R. Roberts, Phys. Rev. A 19, 90 (1979).
[14]G. A. W. Lins, Ph.D. thesis, Ruhr-University, Bochum, W. Germany, 1980 (unpublished).
[15]H. R. Griem, *Plasma Spectroscopy* (McGraw-Hill, New York, 1964).
[16]J. A. Stamper and A. W. DeSilva, Phys. Fluids 12, 1435 (1969).
[17]G. A. W. Lins and H.-J. Kunze, Phys. Fluids, in press.
[18]W. Lotz, Astrophys. J. Suppl. 14, 207 (1967).
[19]A. Burgess, in *Proceedings of the Symposium on Atomic Collision Processes in Plasmas*, Culham AERE Report No. 4818, 63 (1964).
[20]L. B. Golden and D. H. Sampson, J. Phys. B 10, 2229 (1977).
[21]S. M. Younger, Phys. Rev. A 22, 111 (1980).
[22]S. M. Younger, Phys. Rev. A 22, 1425 (1980).
[23]A. H. Gabriel and C. Jordan, in *Case Studies in Atomic Collision Physics* (North-Holland, Amsterdam, 1972), Vol. 2, Chap. 4.
[24]R. C. Elton and W. W. Köppendorfer, Phys. Rev. 160, 194 (1967).
[25]W. L. van Wyngaarden, K. Bhadra, and R. J. W. Henry, Phys. Rev. A 20, 1409 (1979).
[26]A. H. Gabriel and C. Jordan, Mon. Not. R. Astron. Soc. 145, 241 (1969).
[27]D. H. Crandall and R. A. Phaneuf, Phys. Rev. A 18, 1911 (1978).
[28]D. H. Crandall, R. A. Phaneuf, B. E. Hasselquist, and D. C. Gregory, J. Phys. B 12, L249 (1979).